Modeling Sonar Responses of Targets Deployed On or In the Seafloor

Raymond Lim
NSWC PCD, Code X11
110 Vernon Ave
Panama City, FL 32407
Phone: (850) 235-5178 Fax: (850) 235-5374 Email: raymond.lim@navy.mil

Document Number: N0001411WX20015

LONG-TERM GOAL

Recent interest in understanding the potential advantages of nonconventional detection configurations, such as bistatic vs monostatic, has driven efforts to initiate the model refinements needed to study these configurations for simple targets deployed proud or buried on the seafloor. A benchmark quality capability for these targets is utilized so that unambiguous results are available for physical interpretation and analysis, both in laboratory sonar measurements as well as in sonar field tests using the Naval Surface Warfare Center Panama City Division's (NSWC PCD) synthetic aperture sonar (SAS) systems. The long term goal of this effort is to investigate and compare how the physics of a target embedded in a given environment and sensed under different detection modes can affect both target signal-to-noise (SNR) and classification. This knowledge can then be used to improve sonar detection and classification of bottom targets.

OBJECTIVES

One objective is to generate high fidelity datasets to help understand carefully controlled measurements in the scale-model sonar test bed operated at NSWC PCD [1], which can be configured to collect SAS target data along both linear and circular tracks. Interest in circular tracks has grown recently because circular SAS (CSAS) processing may provide imagery with better shape resolution for classification purposes. The comparisons made were used to gain insight to the fidelity of data that can be collected in the test bed by helping to separate target from noise phenomena and by helping to interpret target phenomena that might be useful for target classification. Furthermore, the datasets created are used to study the effectiveness of processing algorithms for isolating signal from noise.

A second objective this year is to test solutions recently proposed by Waterman [2] for stabilizing the spherical-basis T-matrix for nonspherical shapes at high frequencies. This would yield a more practical T-matrix solution than the spheroidal-basis version [3] currently used for elongated shapes, which can still be limited by how accurately high order spheroidal functions can be computed.

APPROACH

For simple near-spherical target shapes proud or buried in a flat ocean bottom, scattering predictions are generated from high-fidelity solutions based on the T-matrix method [4]. Last year [5],

Report Documentation Page

Form Approved
OMB No. 0704-0188

1. REPORT DATE	2. REPORT TYPE	3. DATES COVERED
SEP 2011		**00-00-2011 to 00-00-2011**

4. TITLE AND SUBTITLE	5a. CONTRACT NUMBER
Modeling Sonar Responses of Targets Deployed On or In the Seafloor	5b. GRANT NUMBER
	5c. PROGRAM ELEMENT NUMBER
6. AUTHOR(S)	5d. PROJECT NUMBER
	5e. TASK NUMBER
	5f. WORK UNIT NUMBER
7. PERFORMING ORGANIZATION NAME(S) AND ADDRESS(ES) **Naval Surface Warfare Center (NWCD PCD),Code X11,110 Vernon Ave,Panama City,FL,32407**	8. PERFORMING ORGANIZATION REPORT NUMBER
9. SPONSORING/MONITORING AGENCY NAME(S) AND ADDRESS(ES)	10. SPONSOR/MONITOR'S ACRONYM(S)
	11. SPONSOR/MONITOR'S REPORT NUMBER(S)

12. DISTRIBUTION/AVAILABILITY STATEMENT
Approved for public release; distribution unlimited

13. SUPPLEMENTARY NOTES

14. ABSTRACT

15. SUBJECT TERMS

16. SECURITY CLASSIFICATION OF:			17. LIMITATION OF ABSTRACT	18. NUMBER OF PAGES	19a. NAME OF RESPONSIBLE PERSON
a. REPORT **unclassified**	b. ABSTRACT **unclassified**	c. THIS PAGE **unclassified**	**Same as Report (SAR)**	**9**	

modifications to existing transition (T)-matrix-based buried target scattering codes were carried out to include a capability to model an n-layered elastic sphere deployed proud in a two-halfspace ocean environment and to enable generation of scattering data along linear SAS tracks for both proud and buried configurations. This year, a couple more enhancements were made. The capability to compute the scattering along circular tracks in either halfspace was added so data could be generated for use with CSAS processing algorithms. An existing code for scattering in a layered waveguide [6] was also modified so that scattering can be computed at extended ranges from a target deployed within an environment bounding it from both above and below. The resulting code will be used to study range effects on target signals and features drawn from these signals for classification.

WORK COMPLETED

The T-matrix extensions described above have been written and implemented to run on a desktop computer with a FORTRAN compiler. Tracks for receiver and transmitter motion in circular arcs of specified angular range are allowed and the tracks do not have to coincide, nor are both source and receiver required to move, so bistatic data can be generated. Both the receiver and transmitter can move along independent tracks of different diameter. Although both tracks are assumed centered on the same horizontal coordinates, they may be separated in the vertical direction. As discussed in Ref. 3, the ability to use a phase-steerable, vertically bounded source beam in computations has been built in by encoding the closed form average of the source point, $\mathbf{r}_s$, over a specified vertical source length.

The source can also be allowed to be a plane wave. Data generated for a slightly off-center sphere deployed proud on a sand bottom and detected bistatically with a moving source and stationary receiver has been compared with experimental results from the scale-model test bed and exhibit good agreement. These results are discussed in the test bed annual report.

The modification of the layered waveguide scattering code was done by rotating the integration contours for computing the basis sets and incident field coefficients needed according to the prescription in Ref. [6]. While the previously existing code was usable down to reasonably shallow angles, convergence eventually becomes problematic at the longer ranges desired for sonar operations. This is shown in Fig. 1, for scattering by a 0.5m-diameter, 5% thick, spherical steel shell deployed proud in a 25m-deep planar air/water/sand waveguide. The omnidirectional source/receiver pair is positioned at 3 ground ranges from 25m to 100m from the target at a height of 4m above the bottom. Backscatter intensities are computed with both the previous T-matrix solution (dotted colored lines) and the new one (solid colored lines), optimized for long range. At both 25m and 50m, both solutions agree to within line width and are indistinguishable. However, at a range of 100m, the previous solution is not converged while the new one is, as evidenced by insensitivity to integration parameters.

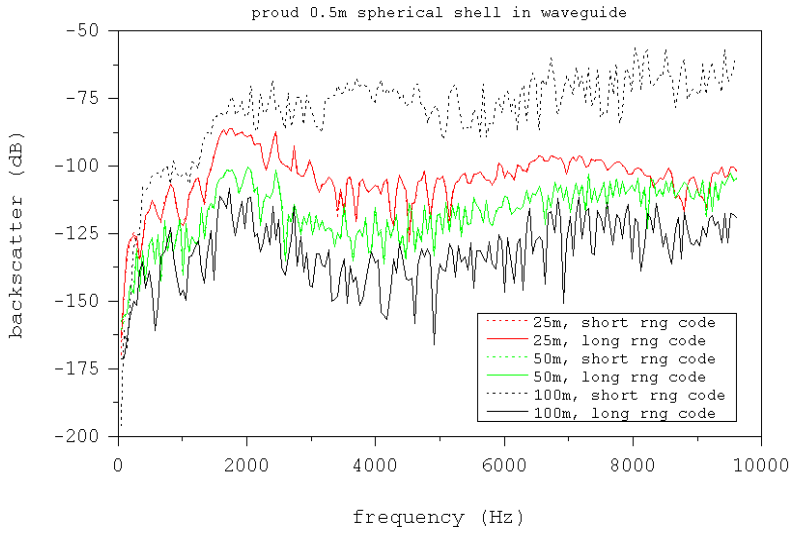

Figure 1. A comparison of backscatter intensity vs frequency computed for a 0.5m-diameter spherical steel shell computed at three ground ranges from the target using the previous-matrix solution optimized for high grazing angles (short range) and the new one optimized for shallow grazing angles (long range).

Solutions to stabilize the spherical-basis T matrix as suggested recently by Waterman [2] were tried but not found to be useful for elastic targets. However, his explanation of the fundamental cause of the instability was found to be valid and is clearly associated with the surface integrals involving high order, irregular spherical functions. As normally formulated, these integrals require very high precision arithmetic to compute accurately for elongated target shapes. However, using arbitrary precision arithmetic software to carry out the many integrals required would be impractical. Alternative formulations that shrink the dynamic range of the integrands through origin translations so the integrations can be performed accurately were also tried but ultimately failed due to poor convergence of the inverse translations that must be applied to the final integrals. Since the difficult surface integrals arise from the use of a spherical mode expansion for the free-field Greens function, it is possible that reformulating parts of the T-matrix without the use this expansion could result in a more stable result. This will be considered in future work.

RESULTS

Processing of forward scattering simulations Because target scattering is known to become dominant in the forward direction as frequency increases [7], notional forward scattering cases were modeled last year to study the difficulties associated with standard beamforming of these configurations. This year, the model simulations carried out last year were used to study the effectiveness and potential artifacts introduced by spatial filters applied to SAS data for removing target forward scatter signals from interference due to direct and bottom bounce source signals. An example considered here is a filter recently suggested by Bucaro *et al.* [8], which essentially time delays unwanted signals till they line up at a particular time and then performs a spatial Fourier transform to project them to low spatial

frequencies where they are selectively filtered out. Such techniques clearly depend on desired and unwanted signals following sufficiently different time delay profiles but they can be quite effective.

To recap the simulations performed last year, computations involved a 0.5m-diameter, 5%-thick stainless steel spherical shell deployed proud on a sand bottom. A point source 4.66m above the sand illuminates the shell from 25m ground range. A point receiver, on the opposite side of the shell from the source, is moved along a 50m track perpendicular to a line going through the source and target. The track is closest to the shell in the center, which is 25m from the shell. The track height above the sand is the same as the source. 250 frequency-point spectra out to 34.2kHz were calculated for both the target strength and the total field (i.e., target + incident field) at each of 403 equally spaced points along the track. These were inverse transformed to produce the time history smiles shown in last year's report and reproduced here in Fig. 2. The limited frequency resolution gives rise to the wrap-around seen in the time domain at the longer ranges, but all relevant features of the target and environment response are present. Field intensity is plotted on a dB scale so the weaker target smile can be seen in the total field time history (Fig. 2(b)). Interference by the bottom bounce is the most problematic issue for isolating the target signal since these two signals are difficult to gate apart.

A useful application of these high-fidelity simulations is to compare filtered target representations against benchmarks created with uncontaminated target signals to gain insight on what effects the filtering process can have. To illustrate, the filter used by Bucaro *et al.* is applied to the complex total field signals used in Fig. 2(b) to remove both the direct path and bottom bounce signals. Filtration of these signals in the spatial frequency domain is performed by convolving with Tukey windows configured with different widths. In Fig. 3(a), the result of filtering out both the bottom bounce and direct path signals is shown using a Tukey window set to remove a spatial frequency band around zero that is 5% of the total band in width. Figure 3(b) shows the result of using a window set to remove 15% of the band around zero to filter out the bottom bounce and a window set to remove 20% of the band around zero to filter out the direct path. While the wider filters remove more of the unwanted signals there is also a modification of some of the secondary structure seen in Fig. 2(a), which represents uncontaminated target scattering.

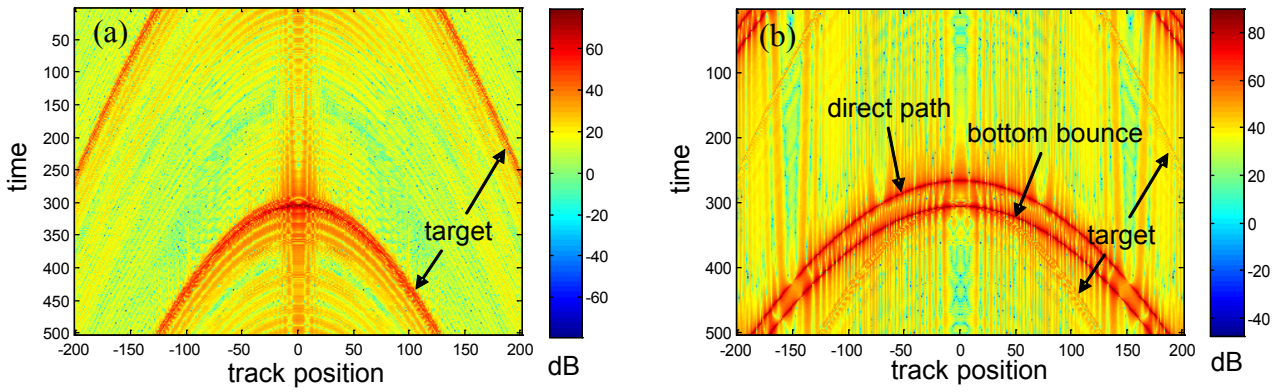

Figure 2. Forward-scattered time histories computed for a proud spherical shell without (a) and with (b) the incident source field. The track position spacing is 0.125m.

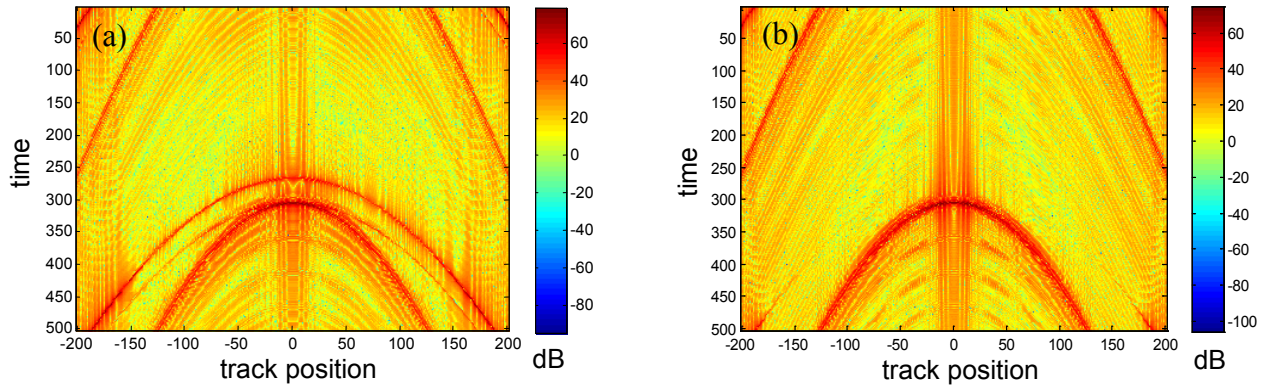

Figure 3. Forward-scattered time histories for a proud spherical shell filtered to remove the bottom bounce and direct path signals using (a) a 5% Tukey window on both signals and (b) a 15% Tukey window on the bottom bounce and a 20% window on the direct path.

While one might initially expect the most complete removal of the direct path and bottom bounce signals to result in better beamformed imagery this is not found to be the case. An image of the sphere resulting from beamforming the uncontaminated signal represented by Fig. 2(a) over a 25m synthetic aperture is shown in Fig. 4. The pixel size is nominally 3.125cm, so the image snippet shows an area of approximately 2.5mx2.5m centered on the shell. In Fig. 5, the result of beamforming the filtered time histories represented in Fig. 3 are shown. The best reproduction of the benchmark is clearly the image formed from beamforming the data with the narrowest filter applied, even though remnants of the unwanted signals are still evident. This is likely due to the beamforming process removing interference remaining from the unwanted signals while more of the target signal not removed by the filtering process is available to improve target imaging. In any case, both filtered images represent a significant improvement over imaging the target by beamforming the raw total forward field.

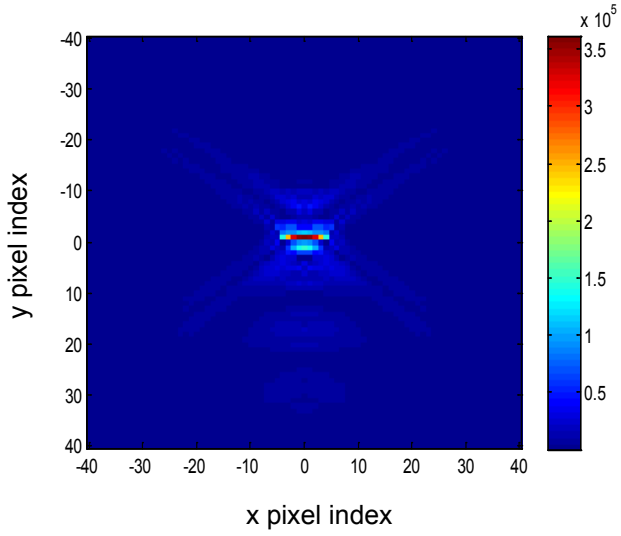

Figure 4. Image snippet centered on a 0.5m-diameter spherical shell deployed proud on a sand bottom and SAS processed using the forward scattered signal without the source field included. The image is processed using a 25m synthetic aperture. The pixel size is nominally 3.125cm.

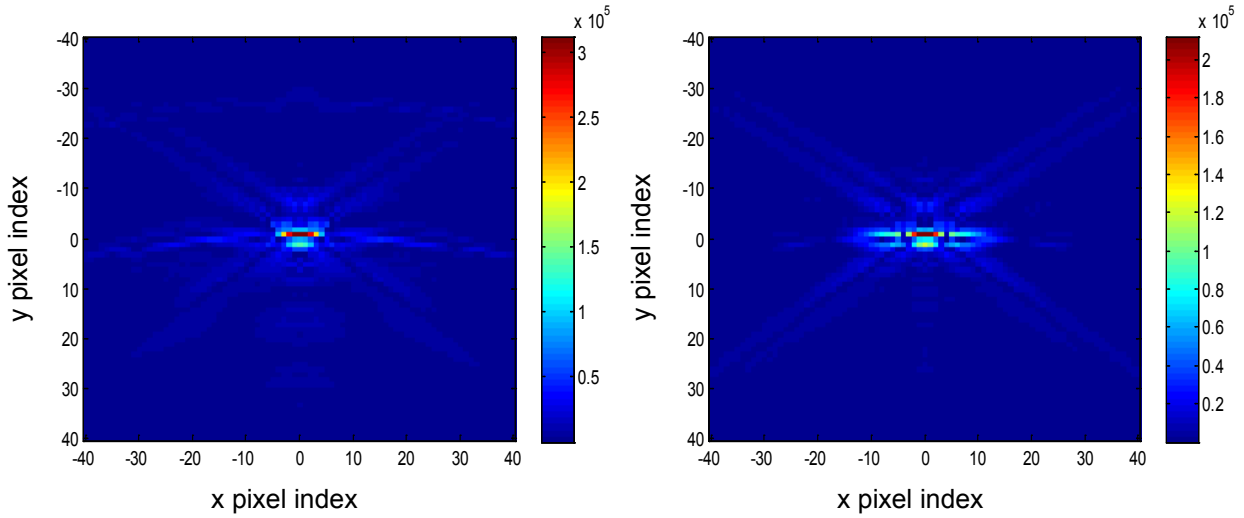

Figure 5. Image snippets of the 0.5m-diameter shell SAS processed using the filtered forward scattered signals depicted in Fig. 3(a) (left) andFig. 3(b) (right).

The effect of the spatial filtering on representations of the target in frequency vs along-track position space can also be compared. In Fig. 6, a spectral intensity plot formed from frequency transforming the time axis of Fig. 2(a) is shown as a benchmark. In Fig. 7, the result of frequency transforming the respective filtered time histories represented in Fig. 3 is shown. In this comparison, it would appear that the better reproduction of the benchmark arises from removing more of the bottom bounce and direct path signals. As expected, degradation occurs near the point of closest approach (track position 0) where contamination of the target signal by the bottom bounce is most severe. Clearly, some trade-offs must be considered to determine the optimal filter parameters to use depending on how one wishes to represent the target.

IMPACT/APPLICATIONS

The updates to scattering models described here form the basis for analyzing measurements, assessing algorithms for automatic target recognition and beamforming, benchmarking future modifications and extensions, and verifying FE algorithms under development. This will lead to improved sonar systems that can detect and identify targets buried over extended ranges in littoral environments.

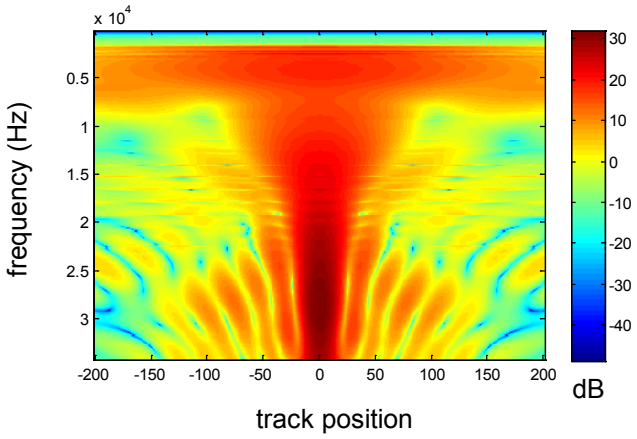

Figure 6. Forward scattered target spectrum vs along-track position determined from the scattered field only.

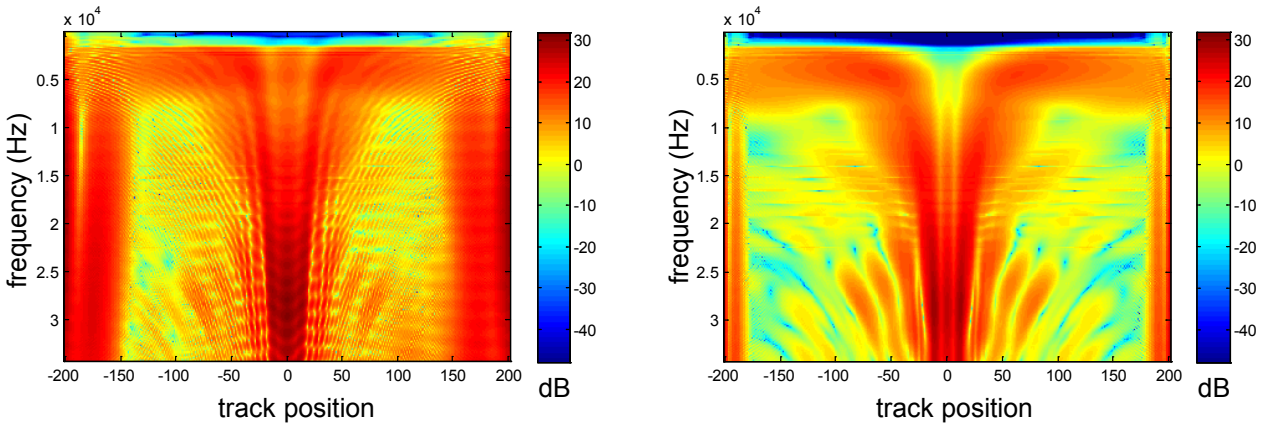

Figure 7. Forward scattered target spectra vs along-track position determined from the filtered total field as depicted in Fig. 3(a) (left) and Fig 3(b) (right) .

TRANSITIONS

These results are being used to understand target signals observed in tests carried out this year and next year with support from ONR's target classification efforts (POC: J. Stack) and to benchmark NSWC PCD's finite element and Personal Computer compatible Shallow Water Acoustic Toolset (PC SWAT) development with support from SERDP's Munitions Management Program (POC: Herb Nelson) and ONR's Data Fusion Program (POC: J. Stack).

RELATED PROJECTS

The present research is closely coordinated with theoretical and experimental efforts ongoing at APL-UW (E. Thorsos and K. Williams) and at NSWC PCD (J. Lopes, D. Burnett) under support from ONR Codes 321OA, 321OE, 321MS, and SERDP to resolve bottom target (mines and UXO) detection issues. D. Burnett is developing a numerical approach based on finite elements to model acoustic scattering and radiation by complex three-dimensional objects near boundaries. The work reported here will play an important role in verifying the resulting models. G. Sammelmann (NSWC PCD) is also continuing to update PC SWAT with algorithms to improve the realism of generated imagery and data sets under support from ONR and SERDP. Related efforts also exist elsewhere. H. Schmidt (Massachusetts Institute of Technology) and coworkers use modifications of the OASES program to predict multi-static scattering by proud and buried targets. J. Fawcett (DRDC-Atlantic, Canada) uses a variety of techniques to develop models of target scattering in layered ocean environments. Other researchers at NURC (A. Tesei, M. Zampolli, Finn Jensen, et al.) are also testing acoustic propagation and scattering models by comparing predictions with data from buried targets and with other benchmark calculations provided at acoustic computation workshops hosted by NURC.

REFERENCES

[1] P. C. Malvoso, J. S. Stroud, R. Lim, J. L. Lopes, B. R. Dzikowicz, "Small scale test bed for studying multiaspect and multistatic sonar systems," *J. Acoust. Soc. Am.* **127**, p. 1748 (2010).

[2] P. C. Waterman, "T-matrix methods in acoustic scattering," *J. Acoust. Soc. Am.* **125**, 42-51 (2009).

[3] R. H. Hackman, "The transition matrix for acoustic and elastic wave scattering in prolate spheroidal coordinates," *J. Acoust. Soc. Am.* **75**, 35-45 (1984).

[4] R. Lim, J. L. Lopes, R. H. Hackman, and D. G. Todoroff, "Scattering by objects buried in underwater sediments: Theory and experiment," *J. Acoust. Soc. Am.* **93**, 1762-1783 (1993).

[5] R. Lim, "Modeling Sonar Responses of Targets Deployed On or In the Seafloor," ONR Ocean Battlespace Sensing FY 2010 Annual Reports (2011).

[6] R. Lim, "Multiple scattering by many bounded obstacles in a multilayered acoustic medium," *J. Acoust. Soc. Am.* **92**, 1593-1612 (1992).

[7] J. A. Bucaro, B. H. Houston, H. Simpson, L. R. Dragonette, L. Kraus, T. Yoder, "Exploiting forward scattering for detecting submerged proud/half-buried unexploded ordnance, *J. Acoust. Soc. Am.* **126**, EL171-176 (2009).

[8] J. A. Bucaro, L. Kraus, B. H. Houston, H. Simpson, A. Sarkissian, "Forward scatter target strength extraction in a marine environment (L)," *J. Acoust. Soc. Am.* **129**, 3453-3456 (2011).

PUBLICATIONS/PRESENTATIONS

R. Lim, J. Kennedy, T. Marston, R. Arrieta, I. Paustian, J. Lopes, "Sonar Measurements and Processing to Facilitate Detection and Classification of Underwater UXO," Partners in Environmental Technology Technical Symposium and Workshop, Washington, D. C., Nov 30-Dec 2, 2010. (poster)

R. Arrieta and R. Lim, "Comparison of time-frequency distributions for target classification," *J. Acoust. Soc. Am.* **129**, p. 2664 (2011). (A)

J. R. La Follett and R. Lim, "Multistatic scattering by scaled metallic targets: Experimental results and modeling," *J. Acoust. Soc. Am.* **129**, p. 2685 (2011). (A)

S. G. Kargl, K. L. Williams, A. L. Espana, J. L. Kennedy, T. Marston, J. L. Lopes, and R. Lim, "Acoustic scattering from underwater munitions near a water-sediment interface," *J. Acoust. Soc. Am.* **129**, p. 2685 (2011). (A)